

A MULTI-WAVELENGTH VIEW ON CORONAL RAIN

D.A.N. Müller^{1,2,3}, A. De Groof⁴, B. De Pontieu⁵, and V.H. Hansteen^{1,2}

¹Institute of Theoretical Astrophysics, University of Oslo, P.O. Box 1029 Blindern, 0315 Oslo, Norway

²Center of Mathematics for Applications, University of Oslo, P.O. Box 1053 Blindern, 0316 Oslo, Norway

³European Space Agency, Research and Scientific Support Department, c/o NASA Goddard Space Flight Center, Mail Code 612.5, Greenbelt, MD 20771, USA

⁴Centrum voor Plasma-Astrofysica, K.U.Leuven, Celestijnenlaan 200B, 3001 Leuven, Belgium

⁵Lockheed Martin Solar & Astrophysics Lab, Palo Alto, 3251 Hanover St., Org. ADBS, Bldg. 252, CA 94304

ABSTRACT

Observations of coronal loops at high temporal resolution reveal their highly dynamic nature. Bright features (“blobs”) suddenly appear in the upper corona and subsequently rain down along arched paths towards the solar surface. The acceleration of these blobs is significantly smaller than free-fall, and some blobs brighten up before reaching the surface. In order to explain these phenomena, we compare $H\alpha$ time series of high-resolution images of coronal rain taken with the Swedish Vacuum Solar Telescope on La Palma with detailed numerical simulations. Our simulations show that any heating mechanism which dissipates energy predominantly at the footpoints of coronal loops is able to trigger a highly dynamic evolution due to a loss of thermal equilibrium at the loop apex. The resulting process of “catastrophic cooling” gives rise to fast downflows of cool, dense plasma blobs which emit strongly in emission lines formed at transition region and chromospheric temperatures. We study the evolution of the observed blobs by tracking the intensities along their paths, and then deduce their projected velocities. From this analysis, we find a good qualitative agreement with the catastrophic cooling model. This finding is supported by data from several other recent observing programs, e.g. an EIT shutterless campaign and a joint observing program (JOP 174) of SOHO and TRACE.

1. INTRODUCTION

The upper solar atmosphere, i.e. the transition region and corona, is highly complex and magnetically structured. Recent space observations, especially with the Solar and Heliospheric Observatory (SOHO) and the Transition Region And Coronal Explorer (TRACE), have revealed that coronal loops, magnetically closed structures in the upper solar atmosphere, are intrinsically dynamic, and intensity enhancements (“blobs”) are often seen to propagate

along these loops. Spectroscopic investigations show that these intensity variations have different signatures in UV spectral lines formed at different temperatures and exhibit Doppler shifts of $v = 20 - 100 \text{ km s}^{-1}$ (Fredvik et al. 2002). In an overview of observations of the temporal variability of active region loops with the Coronal Diagnostic Spectrometer (CDS), Kjeldseth-Moe & Brekke (1998) report significant changes of coronal loops over a period of one hour, in particular seen in emission lines in the temperature range between $T = 1 - 5 \cdot 10^5 \text{ K}$.

Recently, De Groof et al. (2004) observed propagating intensity variations in the He II 30.4 nm band with the Extreme-Ultraviolet Imaging Telescope (EIT). The dominant part of the plasma emitting in this spectral band has temperatures of $T = 6 - 8 \cdot 10^4 \text{ K}$. Plasma seen in this spectral band in higher layers of the solar atmosphere is thus considerably cooler than its surroundings. This can be the result of plasma draining from a prominence or material cooling down after a flare. However, when evidence for these two processes is lacking, the nature of these intensity variations is difficult to explain. While slow magneto-acoustic waves may in general account for propagating intensity variations, this explanation of the features observed in the EIT shutterless campaign from 11 July 2001 was ruled out by De Groof et al. (2004).

A possible explanation is given by the catastrophic cooling/evaporation-condensation cycle model (Müller et al. 2003, 2004, 2005). In these papers we showed that localized brightenings can be the result of catastrophic cooling of a loop which is predominantly heated at the footpoints. The heating leads to an evaporation of plasma into the coronal loop which then cools rapidly due to a loss of thermal equilibrium. The confined region of “condensed” plasma subsequently falls down under the effect of gravity in the form of a cool plasma blob.

2. NUMERICAL MODEL

We use the same numerical model as in Müller et al. (2003), and the reader is referred to this work and to Müller (2004) for details. Our code solves the one-dimensional time-dependent hydrodynamic equations for mass, momentum and energy conservation, coupled with the ionization rate equations for several elements and self-consistent radiative losses. The plasma is assumed to be effectively thin, and the radiative losses are due to collisional excitation of the various ions comprising the plasma, in addition to thermal bremsstrahlung. Thermal conduction, radiative losses and a coronal heating term are included in the energy equation. In the radiative losses the elements hydrogen, helium, carbon, oxygen, silicon, neon, and iron are included. While some of the metals are treated by assuming ionization equilibrium and then deriving an *a priori* radiative loss curve as a function of electron temperature, radiative losses from hydrogen, helium, carbon and oxygen are computed consistently with full time-dependent rate equations. We consider a loop of low- β plasma and assume that the loop has a constant cross section.

The energy input into the coronal loop is parametrized by specifying the energy flux at the footpoints of the loop, F_{m0} , and assuming a mechanical energy flux that is constant up to a height z_1 and then decreases exponentially for $z \geq z_1$ as

$$F_m(z) = F_{m0} \exp[-(z - z_1)/H_m] \quad (1)$$

with a damping length H_m , a mechanical energy flux $F_{m0} = c \cdot 10^4 \text{ W/m}^2$ (with the normalization constant $c = 1/(1 - \exp[-(L/2 - z_1)/H_m])$) and $z_1 = 1.75 \text{ Mm}$.

In Müller et al. (2005), we described how a short damping length (around $H_m = 2 - 5 \text{ Mm}$) can lead to “coronal rain”, i.e. fast downflows of dense plasma blobs. An exponentially decaying heating function was first suggested by Serio et al. (1981) and seems to be supported by recent observations (Aschwanden et al. 2000, 2001) as well as by numerical simulations of Gudiksen & Nordlund (2002). Aschwanden et al. (2001) find that a damping length $H_m = 12 \pm 5 \text{ Mm}$ yields the best fit of hydrostatic models to TRACE observations, while 70% of the observed loops are not compatible with hydrostatic models at all. This indicates that time-dependent models are indeed needed to understand the evolution of coronal loop plasma.

3. OBSERVATIONAL DATA

On May 26, 2000, time series of filtergrams were obtained with the Swedish Vacuum Solar Telescope (SVST) on La Palma. The field-of-view was centered on the solar limb which makes it possible to study low-temperature plasma in coronal loops above the limb. The data consist of four series of filtergrams in the blue and red wing of the

$H\alpha$ (6563 Å) line ($\lambda_0 \pm 350 \text{ mÅ}$ and $\lambda_0 \pm 700 \text{ mÅ}$, FWHM 100 mÅ) and a time series of filtergrams in the Ca II K (3933 Å) line, each taken between 12:00 and 18:00 UT.

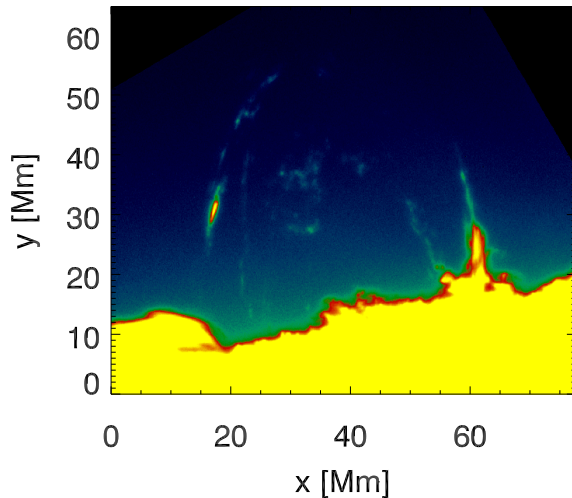


Figure 1. This overexposed image shows bright blobs of plasma seen in the blue wing of the $H\alpha$ line ($\lambda_0 - 350 \text{ mÅ}$), which are moving towards the solar surface.

Fig. 1 shows an image taken at 14:31 UT in the blue wing of the $H\alpha$ line ($\lambda_0 - 350 \text{ mÅ}$). In this overexposed display, several bright features can be seen which outline the left half of a coronal loop structure. Combining the data from all four wavelengths, a large number of coronal loop structures can be identified. A selection of these coronal loops, along which bright blobs are observed to move towards the solar surface, is overlaid in Fig. 2.

The primary goal of this study is to infer the speeds at which these bright features move. We will also propose a mechanism which offers an explanation for the different speeds which are observed. The work presented in this study is complementary to the work by De Groof et al. (2005b), and we refer the reader to this work and to De Groof et al. (2005a) for a detailed analysis of co-registered data sets taken with EIT in the 30.4 nm pass-band and Big Bear $H\alpha$ data.

In this work we will only deduce the projected velocities of the moving features. It should be noted that these projected velocities are lower bounds for the true velocities. A combination of the data from the four wavelengths in the $H\alpha$ line with a geometrical loop model could help to obtain a more accurate estimate of the true velocities (this will be done in a future piece of work).

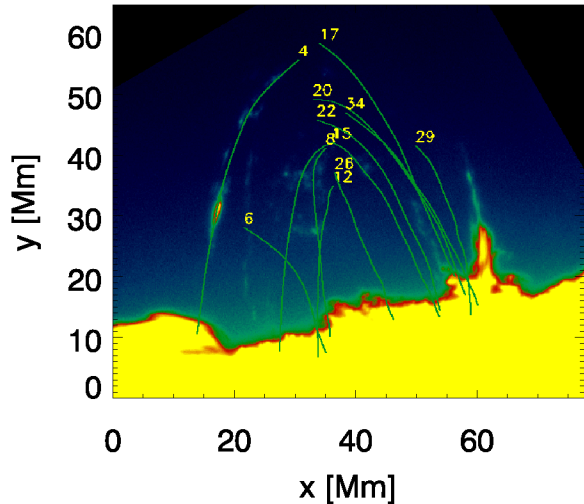


Figure 2. The same overexposed image as in Fig. 1. Overlaid is a selection of coronal loops, along which bright blobs are observed to move towards the solar surface. The loops have been identified using data from all four wavelength positions in the $H\alpha$ line.

4. DATA ANALYSIS AND COMPARISON WITH HYDRODYNAMIC MODELS

In order to measure the projected velocities, the following procedure was used: First, several points along the loop structures were identified by hand, and then a spline interpolation was performed to trace the loops' shapes smoothly. After that, the intensities along the traces were extracted for all frames and all four wavelengths. These time series of intensities were then assembled to space-time diagrams by interpolating the data to a common regular grid in time. As an example, Fig. 3 shows the space-time plot for loop structure no. 4, observed in the blue wing of the $H\alpha$ line ($\lambda_0 - 350 \text{ m}\text{\AA}$).

In these diagrams, moving bright blobs show up as bright ridges. If intensity enhancements which move along different paths are crossing the loop trace by chance, they also show up as bright features in the space-time diagram (e.g. in the right half of Fig. 3), but prominent ridges will only appear when the intensity enhancements are moving along the coronal loop, which makes it easy to separate the two phenomena.

From these space-time diagrams, the projected velocities of bright moving features (“blobs”) were calculated by measuring the slope of the bright ridges. While a detailed analysis of the velocities deduced from all data sets will be presented in a forthcoming paper, we focus in this contribution on the observation confirmation of a specific phenomenon which has been described in Müller et al. (2005). It turns out that in the catastrophic cooling/evaporation-condensation cycle model, the highest blob velocities are observed when a plasma blob trav-

els in the wake of another one. In this case, the plasma density in front of the second blob is decreased due to the fact that most of the plasma has been swept up by the first blob. As a consequence, the pressure downstream of the second blob is much smaller so that the blob's acceleration reaches almost free-fall values. This results in the second blob moving at much higher velocities than the first one, which feels a stronger counterpressure of the transition region plasma below it.

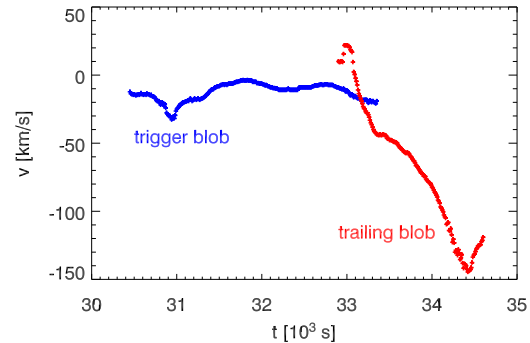


Figure 4. Blob velocity extracted from a hydrodynamic simulation of a 300 Mm model loop.

Fig. 4 shows the blob velocities extracted from a hydrodynamic simulation of a 300 Mm model loop. While the first blob, labeled as “trigger blob” (blue crosses) reaches a maximal velocity of about 35 km/s, the second blob (labeled as “trailing blob”, red crosses) is accelerated to up to 145 km/s. Depending on the exact treatment of the non-equilibrium ionization, the maximal speeds obtained vary between 90 km/s and 150 km/s as the condensation regions form at slightly different heights in the coronal loop.

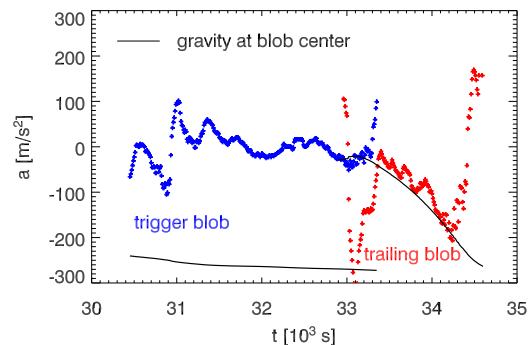


Figure 5. Blob acceleration corresponding to the velocity plot in Fig. 4. The black lines indicate the effective gravitational acceleration of the blob (g_{\parallel}) as it moves along the model loop.

Fig. 5 shows the blobs' acceleration corresponding to the

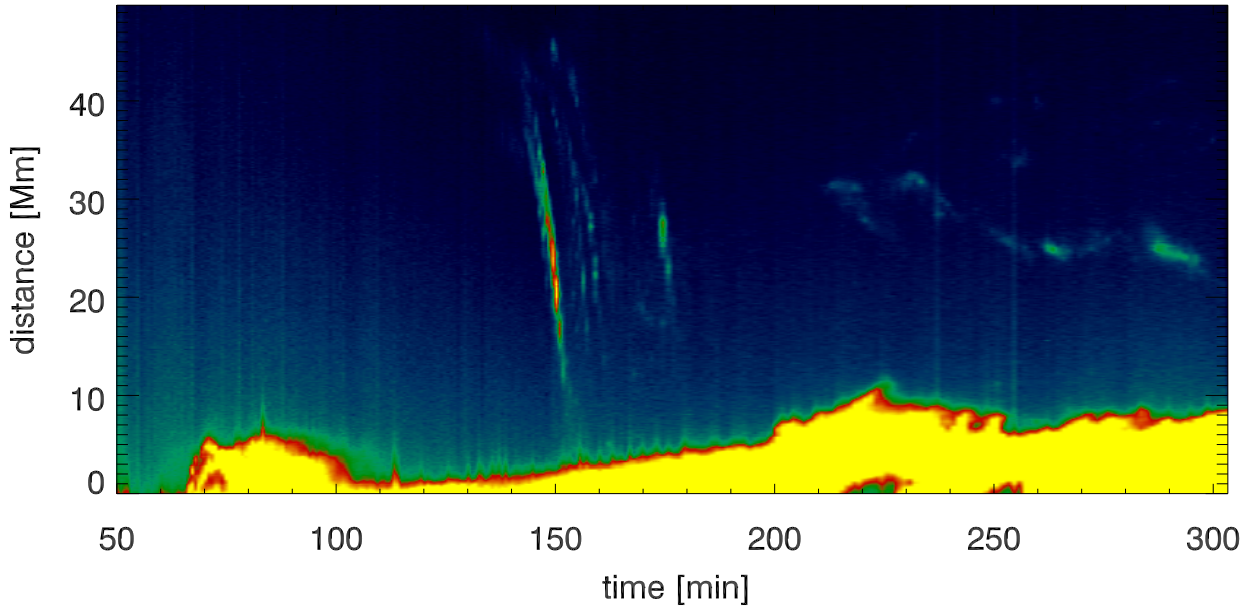


Figure 3. Space-time plot of emission in the blue wing of the $H\alpha$ line ($\lambda_0 = 350 \text{ mÅ}$) along coronal loop no. 4 (see Fig. 2). The bright ridges in the space-time plot correspond to “blobs” moving downwards along this loop.

velocity plot in Fig. 4. The black lines indicate the effective gravitational acceleration of the blob (g_{\parallel}) as it moves along the model loop. This plot illustrates how strongly the first blob is decelerated by the underlying plasma while the second blob is accelerated by nearly the full gravitational acceleration along the loop (g_{\parallel}).

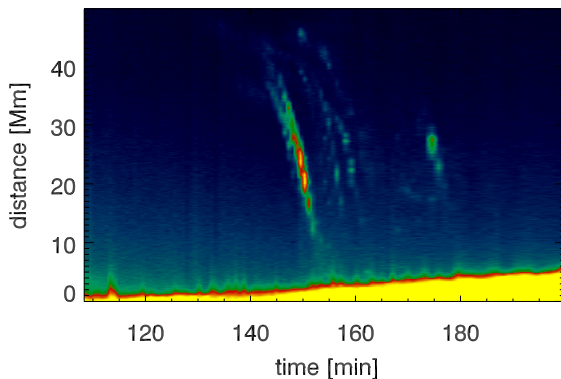


Figure 6. Close-up of Fig. 3. The bright structure on the left consists of two ridges which eventually merge close to the solar surface.

To compare this prediction with observational data, we show in Fig 6 a close-up of the bright ridges seen in the left part of Fig. 3. The plot reveals two ridges with different slopes which eventually merge close to the solar surface. The first one has a shallower slope, corresponding to a projected velocity of up to 65 km/s, while the slope of the second ridge corresponds to a velocity of up

to 125 km/s.

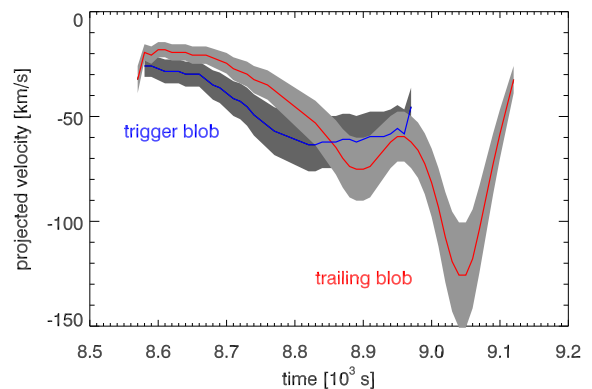


Figure 7. Projected velocity deduced from the slope of the ridges in the space-time plot in Fig. 6. The blue line shows the velocity of the first feature (“trigger blob”), the red line that of the second one (“trailing blob”). The shaded areas indicate a preliminary estimate of the measurement uncertainties of 20%.

Fig. 7 displays the blobs’ projected velocities as a function of time, along with a preliminary error estimate of 20%. In agreement with the model, it is seen that indeed one blob follows another one, and that the second blob travels at significantly higher speed than the first one. Since this particular hydrodynamic model has a loop length of 300 Mm, which is significantly longer than the observed loop, the time scale on which the second blob is following the first one is longer than that seen in the ob-

servational data. Furthermore, a quantitative comparison of the blob speeds require a three-dimensional geometric model of the loop to infer its aspect angle with respect to the observer. While further investigation is needed to find out how common this process is and what the range of observed velocities are, we report here for the first time the observation of the predicted phenomenon of leading/following blobs at slow and high speeds.

5. FUTURE WORK

Combining the $H\alpha$ data with the data taken with the Ca II K (3933 Å) filter, we will try to follow the cooling process of the plasma down to chromospheric temperatures. Furthermore, a comparison with the simultaneous data taken with TRACE in the 1600 Å passband will help to determine the initiation of the cooling process. For a detailed analysis of the TRACE data, the reader is referred to Schrijver (2001).

6. SUMMARY

In this work, we have presented a first comparison between $H\alpha$ filtergrams obtained from the Swedish Vacuum Solar Telescope on La Palma and 1D-radiation-hydrodynamic models. We report here for the first time the observation of the predicted phenomenon of leading/following blobs at slow and high speeds in coronal loops. We find evidence for bright blobs in coronal loops moving at speeds of more than 100 km/s. These blobs appear in the wake of another blob which is moving at significantly lower speed. Our hydrodynamic models suggest that this phenomenon is due to the fact that the first blob is strongly decelerated by the underlying plasma of the transition region, while the second blob can move unobstructedly in its low-pressure wake. The origin of the second blob is the compression of the loop plasma due to a shock associated with the formation of the first blob. The combination of observations and models provides strong evidence that coronal loops are indeed heated in the low corona. Furthermore, many of the observed phenomena can be explained on the basis of the catastrophic cooling model.

ACKNOWLEDGMENTS

This work was supported by the EU-Network HPRN-CT-2002-00310.

REFERENCES

Aschwanden, M. J., Nightingale, R. W., & Alexander, D. 2000, *ApJ*, 541, 1059

Aschwanden, M. J., Schrijver, C. J., & Alexander, D. 2001, *ApJ*, 550, 1036

De Groof, A., Bastiaensen, C., Müller, D. A. N., Berghmans, D., & Poedts, S. 2005a, *A&A*, in press

De Groof, A., Berghmans, D., van Driel-Gesztelyi, L., & Poedts, S. 2004, *A&A*, 415, 1141

De Groof, A., Müller, D. A. N., & Poedts, S. 2005b, these proceedings

Fredvik, T., Kjeldseth-Moe, O., Haugan, S. V. H., Brekke, P., Gurman, J. B., & Wilhelm, K. 2002, *Adv. Space Res.*, 30, 635

Gudiksen, B. V. & Nordlund, Å. 2002, *ApJ*, 572, L113

Kjeldseth-Moe, O. & Brekke, P. 1998, *Sol. Phys.*, 182, 73

Müller, D. 2004, PhD thesis, University of Freiburg

Müller, D. A. N., de Groof, A., Hansteen, V. H., & Peter, H. 2005, *A&A*, 436, 1067

Müller, D. A. N., Hansteen, V. H., & Peter, H. 2003, *A&A*, 411, 605

Müller, D. A. N., Peter, H., & Hansteen, V. H. 2004, *A&A*, 424, 289

Schrijver, C. J. 2001, *Sol. Phys.*, 198, 325

Serio, S., Peres, G., Vaiana, G. S., Golub, L., & Rosner, R. 1981, *ApJ*, 243, 288